SHAPE OPTIMIZATION OF HELICAL COIL TUBE FOR MAXIMIZING HEAT TRANSFER

by

VENKAT MANOJ KANDUKURI

Presented to the Faculty of the Graduate School of

The University of Texas at Arlington in Partial Fulfillment

of the Requirements

for the Degree of

MASTER OF SCIENCE IN MECHANICAL ENGINEERING

THE UNIVERSITY OF TEXAS AT ARLINGTON

FALL 2016

Acknowledgements

Firstly, I would like to express my sincere gratitude to my advisor Dr. Brian Dennis, who gave me an opportunity to be a part of CFDLAB at UTA and encouraged me with the spirit of independent and instilled a research by giving access to all possible resources. This research would not have been possible without his exceptional guidance.

Besides my Advisor, I would like to thank my committee members Dr. Bo. P. Wang and Dr. Han from Mechanical and Aerospace Department. I would like to take this opportunity to thank Siddarth Chintamani, Sandeep Patel and James Grisham for their advising hours and reviewing towards my thesis.

Finally, I am thankful to my family and friends back home for sticking me through and helping me out in every possible way. I also grateful to all my past and present teachers who have played a role in shaping up my career.

Above all, I would like to express my deepest gratitude to my parents Gopala Rao Kandukuri and Anuradha Kandukuri, to whom I owe my existence and who made me a good human being.

December 21, 2016

ABSTRACT

SHAPE OPTIMIZATION OF HELICAL COIL FOR MAXIMIZING HEAT TRANSFER

VENKAT MANOJ KANDUKURI, MS

The University of Texas at Arlington, 2016

Supervising Professor: Brian Dennis

Many researchers have observed the enhancement of heat transfer in coiled tubes compared to straight tubes with the same diameter and length. It is known fact, that in a helical coil tube the maximum axial velocity shifted towards the outer wall of the pipe and imbalance between centrifugal forces and inertial loads to a secondary motion of the fluid in the cross-section of the tube. This secondary motion is responsible for improved transport of heat energy to/from the tube walls. Previous conducted Experimental and computational parametric studies show the relationship between the increased heat transfer and parameters such as pitch, coil diameter, Dean's and Reynolds numbers subjected to different boundary conditions. The majority of these studies have focused on tubes with circular cross-sections.

In the present work, a comprehensive parametric study involving a complete set of non-dimensional parameters has been performed for laminar flow using computational fluid dynamics. The non-dimensional parameters governing the flow through the helical tube are the Reynolds number based on hydraulic diameter, Prandtl Number, the ratio of the helical coil diameter to the tube diameter, the ratio of pitch to the tube diameter, and the ratio of the tube length to the tube diameter. In a separate study, the cross-sectional shape was found to have an impact the heat transfer performance. In order to find the optimal cross-sectional shape and other geometric parameters that maximize the heat transfer performance, shape optimization was carried using a numerical optimization algorithm. 45.9% increase in heat transfer was obtained with the optimized shape, when compared to a straight tube and increase by 5% when compared to helical coiled tube with circular cross section.

TABLE OF CONTENTS

LIST OF ILLUSTRATIONS

LIST OF TABLES

CHAPTER 1 INTRODUCTION

1.1 Flow in Helical Tubes

1.1.1 Secondary Flow and its Features in Helical Coiled Tube

It has been known fact that when fluid flows in a helical coil tube, there is a significant losses which are greater than those compared with straight tube. There must be a phenomenon of secondary flow present in the tube which is not there in a Straight pipe. When fluid flows in a curved tubes, secondary flow are induced due to centrifugal forces generated due to the curvature of curved tubes, which has an ability to enhance the heat transfer performance.

The secondary flow pattern consists of two perpendicular vortices to the axial flow direction. The convective heat transport is more or less depending on the flow parameters and fluid properties. The secondary flow caused due to the centrifugal forces generates a circular motion which moves the fluid particles towards the core region of the tube. As the fluid flow rate increases the intensity of the secondary flow increases. Laminar flow regime persists for much higher Reynolds number for helical tube than that of straight tube due to stabilizing effects of the secondary flow caused due to the curvature of the helical pipe.

Different studies were conducted in the past on fluid flow in helical coils with circular cross-sections, in order to understand the effect of geometry on the heat transfer through the coil tube walls. Heat Transfer and flow in curved pipe was comprehensively studied by Berger [1], reported the structure of velocity and

temperature fields and the form of dependency of geometrical parameters on these fields. Different design correlations were developed for friction factor by many researchers, with applicability was restricted to geometrical and flow conditions. Dean [2] analyzed toroidal pipes analytically developing a mathematical expressions for induced effects of geometry on axial velocity and pressure fields and used Reynolds number and D/d to correlate the geometric parameters to the flow conditions. Schmidt and Micheeff gave empirical relations for overall heat transfer coefficient in case of a constant wall temperature. In case of a fully thermal region of uniform heat flux, Dravid[6], seban and Mclaughlin[8] gave the empirical formulae for local averaged heat transfer coefficient. Numerical study was reported by Patankar [9], Akiyama [10], and Jayakumar [11].

Patankar [9] conducted a comprehensive study to gain an insight and relation between the heat transfer and hydrodynamics of laminar flow in coiled tubes. The laminar flow regime was divided into regions based on non-dimensional parameter Dean number, $De=Re*(d/D)^{0.5}$. They divided into 3 regions, a) small De, De < 17 b) Intermediate De, 17 < De < 100 c) High De, De>100.

In the region of small Dean numbers (De <17), inertia forces can be neglected and secondary vortices are proportional to De^2. In the intermediate Dean number region the inertia forces are balanced with the viscous forces and secondary vortices are proportional to De. For Dean number higher than 100, the

boundary layer flow near the tube wall have significant viscous forces and in the core region away from the wall, secondary vortices are approximately proportional to $De^{1/2}$. The velocity distributions had a good argument with the equations described in Dean [13] and Mori and Nakayama [14].

Austen [15] conducted experimental analysis on laminar heat transfer to explore the pitch effects and reported the effect of pitch on wall temperatures, Nusselt number are substantial for low Reynolds numbers and diminishes as the Reynolds number increases. These effects accredited to free convection, which becomes notable for low pitch helical tubes at low Reynolds number, where secondary flow field due to centrifugal forces is weak. Jayakumar [11] reported experimental and numerical analysis of non-isothermal fluid flow and heat transfer under turbulent fluid flow regime through helical coils with both constant wall temperatures and constant wall heat flux boundary conditions under the influence of Coil diameter, pitch and pipe diameter. Report concluded that, for a constant Reynolds number, heat transfer and pressure drop decreases as coil diameter increases. As the pitch increases, higher temperature regions are observed on bottom half of the pipe. Zapryanov [16] studied numerically using fraction steps on hydrodynamics and thermal problems for fully developed steady laminar incompressible flow through a curved pipe. Results from the numerical methods shows a good argument on axial velocity profiles and temperature profiles from low to high dean and Prandtl number.

Numerical model was presented by Yang et al [17] to study the laminar convective hear transfer for a fully developed flow in a helicoidally pipe with finite pitch. Effects of torsion, Prandtl number and Dean number on laminar convective heat transfer was discussed. Pipe was assumed to have uniform peripheral wall temperature along with uniform axial heat flux. Results shows that gradient of temperature increased on 1 side of the pipe wall and decreased on other side due to increase in torsion. At high Prandtl number, Nusselt number decreased significantly as torsion increased and at low Prandtl number Nusselt number slightly decreased as torsion increased.

The effect of buoyancy forces on secondary flow and heat transfer was studied in a helically coiled heat exchanger by Sillekens et al [18]. Results showed that, for flow in a helically coiled tube with constant wall temperature, secondary flow due to centrifugal forces and buoyancy forces affected the heat transfer rate. Williams [19] reported that the maximum axial velocity shifted towards the outer wall of the pipe and imbalance between centrifugal forces and inertial leads to a secondary motion of the fluid in the cross-section of the pipe.

1.1.2 Design Optimization

Optimization is becoming an important tool in different fields of study, from engineering to finances. For example scientists use optimization to obtain the best element from the models and analyze the phenomenon, engineers use optimization to get best factors to improve the output of a process. Optimization

gained its importance in recent years due to the computer revolution, which led to the development of linear programming and then to the interior point algorithms. George B Dantizig proposed the simplex method in 1947. Linear and non-linear solution methods are developed by convex optimization which have more properties and guarantee that the optimized value is a local and also a global point.

The general problem (GP) description,

$$\min f(x) \qquad \text{Equation [1]}$$

Subjected to

$$g_i(x) = 0 \quad \text{Where i= 1, 2, 3, 4, 5,….m}_a$$

$$g_i(x) \leq 0 \text{ Where j=m}_a\text{+1,…, m}$$

Where x is the vector of n design variables. $f(x)$ is the objective function

General steps for the optimization

1. Estimate the objective function at initial point X^0. Set it to iteration counter =0
2. Compute the direction search d^k for the k^{th} iteration
3. Check the convergence of the objective function
4. Calculate the step size α_k in the direction of d^k
5. Update X for the K+1 iteration by adding the step size to the X values of previous iteration in the search direction

$$X^{k+1} = X^k + \alpha_k d^k$$

6. Go to step 2 and continue until convergence is achieved.

In this present study Matlab's constraint non-linear optimization with Active set algorithm was used, which utilizes the quasi newton's method as a sub process which solves the sufficient and necessary conditions given by Karush Kuhn Tucker to find an optimum. Quasi newton method calculates the Hessian of the objective function using finite difference method to obtain the search direction Arora, J. [21] described the iterative procedure for optimization using Active-Set algorithm as ,

Step 1: Estimate the initial design with initial guess $X^{(0)}$. Choose the system of positive definite n x n matrix $H^{(0)}$ as an estimate for Hessian of the objective function. In absence of more information, Let $H^{(0)}$ = I. select a convergence parameter ε. Set K = 0 and compute the gradient vector as

$$e^{(0)} = \nabla f(X^{(0)}) \qquad \text{Equation 1(a)}$$

Step 2: Calculate the norm of the gradient vector as $\left\|e^{(k)}\right\|$. If $\left\|e^{(k)}\right\| < \varepsilon$ then stop the iterative process, otherwise continue.

Step3: Solve the linear system of equations $H^{(k)}d^{(k)} = e^{(k)}$ to obtain the search direction $d^{(k)}$ for the objective function towards the optimum.

Step4: Compute the step size α_k to minimize $f(X^{(k)} + \alpha_k d^{(k)})$ Equation 1(b)

Step5: Update the design initial guess as $X^{(k)} + \alpha_k d^{(k)}$ Equation 1(c)

Step6: Update the Hessian approximation for the objective function as

$$H^{(k+1)} = H^{(k)} + D^{(k)} + E^{(K)} \quad \text{Equation 1(d)}$$

Where the correction matrices $D^{(k)} and\ E^{(K)}$ are given as

$$D^{(K)} = \frac{Y^{(k)} Y^{(k)^T}}{Y^{(k)}.S^{(k)}} \quad \text{Equation 1(e)}$$

$$E^{(K)} = \frac{C^{(k)} C^{(k)^T}}{C^{(k)}.d^{(k)}} \quad \text{Equation 1(f)}$$

$$S^{(k)} = \alpha_k d^{(k)} \ (change\ in\ design) \quad \text{Equation 1(g)}$$

$$Y^{(k)} = e^{(k+1)} - e^{(k)} \ (change\ in\ Gradient) \quad \text{Equation 1(h)}$$

$$e^{(k+1)} = \nabla f(X^{(k+1)}) \quad \text{Equation 1(i)}$$

Step7: Set k=k+1 and go to step 2.

1.1.3 Thesis Structure

Thesis consists of Introduction Chapter 1 describing literature survey of flow in a helical coil tube and also referring to some of the previously published Optimization related work.

Chapter 2, describes the Geometry and Numerical method used for the study.

Chapter 3, presents comprehensive parametric study involving a complete set of non-dimensional parameters have been performed for laminar flow in a helical tube using computational fluid dynamics.

Chapter 4, presents Shape Optimization of helical coil tube was done with considering Geometrical parameters as design variables.

Chapter 5, conclusions and Future work

CHAPTER 2 GEOMETRY AND NUMERICAL METHOD

2.1 Geometry

The helical coil is typically defined by a helix, as axis of rotation. The helix is defined by the Curvature, Pitch and rotational direction. Pitch is the distance between 2 consecutive turns of the helix. Curvature is related to the diameter of the helix from the axis of rotation. The parametric equations defining helix are given by

$$X(t) = a * \cos t \quad \text{Equation 2(a)}$$

$$Y(t) = a * \sin t \quad \text{Equation 2(b)}$$

$$Z(t) = b * t \quad \text{Equation 2(c)}$$

$$t \in [0, N]$$

Where,

$a = Helix\ Radius$

$\mathrm{b} = \mathrm{Pitch}/2\pi$

$$\mathrm{N} = \frac{L}{\sqrt{a^2 + b^2}}$$

$\mathrm{L} = \mathrm{Arc\ length\ of\ the\ Helix}$

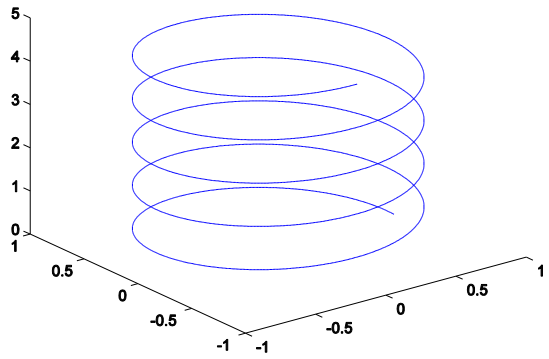

Figure 1 Helix diagram

The shape of the cross-sectional tube is defined by Super ellipse equation. Super ellipse is a curve with Cartesian equation as given in Equation 3. Where A, B are the Major and minor axis of the super ellipse curve and 'n' is the shape power factor.

$$\left(\frac{X}{A}\right)^n + \left(\frac{Y}{B}\right)^n = 1 \qquad \text{Equation 3}$$

Lame` parameterized the super ellipse equation by

$$X = A * cos^{\frac{2}{n}}t \qquad \text{Equation 3(a)}$$

$$Y = B * sin^{\frac{2}{n}}t \qquad \text{Equation 3(b)}$$

Super-ellipses with A=B are known as Lame` family of curves and circle is in Lame` family of curves with n=2.

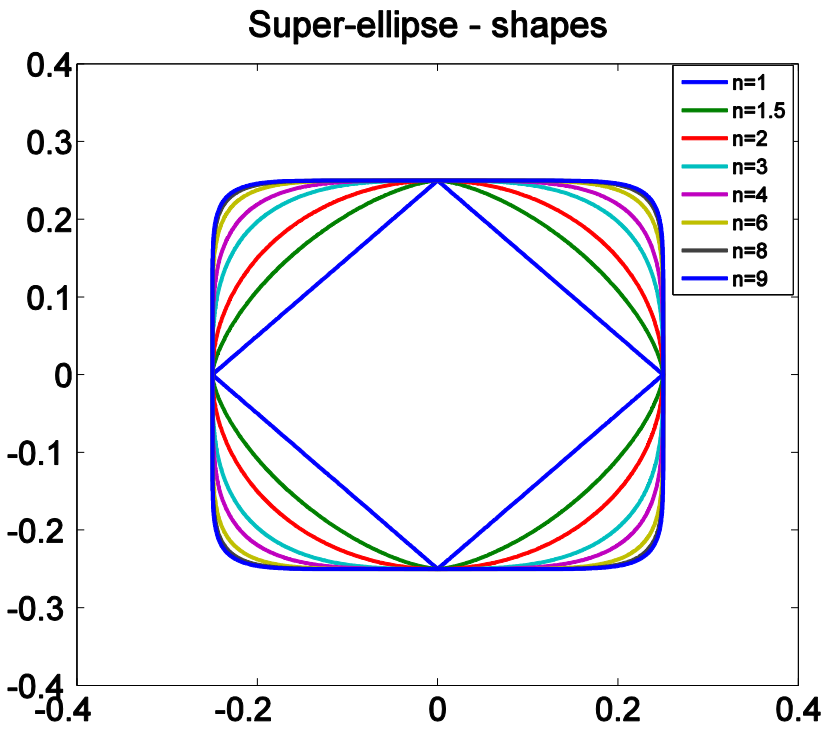

Figure 2 Super-ellipse shapes with varying Shape power factor (n)

The geometric parameters of helical coil are non-dimensional by parameterizing with tube diameter (d), G1 Ratio of length to tube diameter ($\frac{L}{d}$), ratio of Pitch to tube diameter G2 ($\frac{P}{d}$) and G3 ratio of Coil diameter to tube diameter ($\frac{\mathrm{D_{coil}}}{d}$). Curvature ratio is defined by tube diameter to coil diameter ($\frac{d}{\mathrm{D_{coil}}} = \delta$). K_{ab} is ratio of diameter of major axis to minor axis of the cross-sectional shape ($\frac{A}{\mathrm{B}}$). K_c is ratio of coil diameter to diameter of major axis of the cross-sectional shape ($\frac{\mathrm{D_{coil}}}{2\mathrm{A}}$). K_P is ratio of pitch to diameter of minor axis of the cross-sectional shape ($\frac{P}{2\mathrm{B}}$)

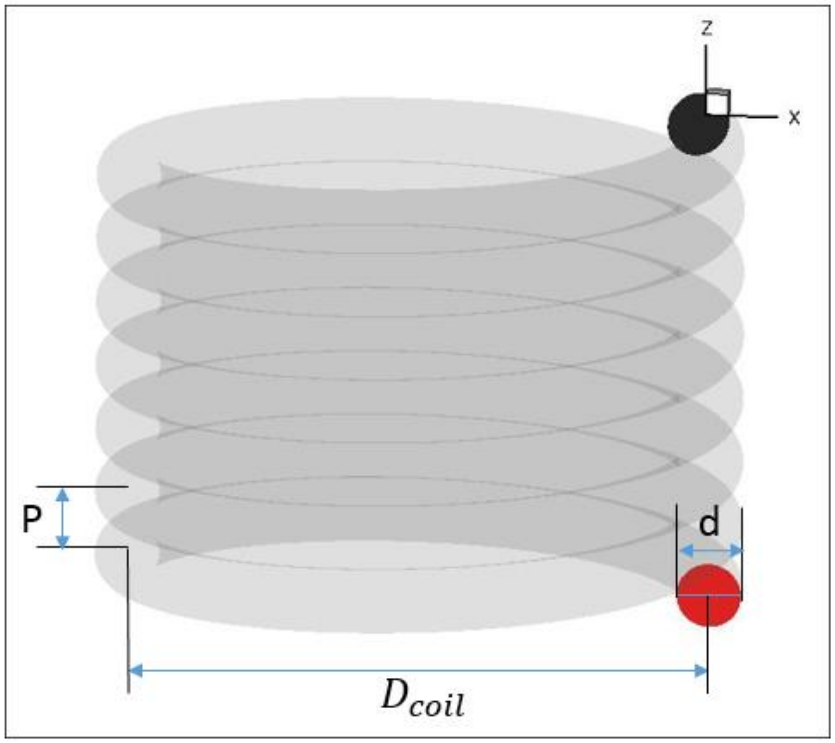

Figure 3 Schematic Diagram for helix pipe

2.2 Grid Generation

After the Helical coil Geometry had been defined, the next step was to discretize the computational domain as a pre-processor in the numerical analysis. For the computational and numerical accuracy, a structural mesh has been used and were generated using pointwiseV17.0R2. The scripting capabilities of the pointwise were used while generating the grids. A pointwise script was written in Glyph2, based on tcl which constructs the structural O-H grid topology based on defined geometric parameters such as radius of major axis and minor axis of tube cross-section, radius, length and pitch of the helical coil and grid dimensions. The Grid

dimensions are given as radial dimensions for interior block along radial direction and tangential dimension for circle and square. These are described in Figure 4. The automated script also exports the file for the solver.

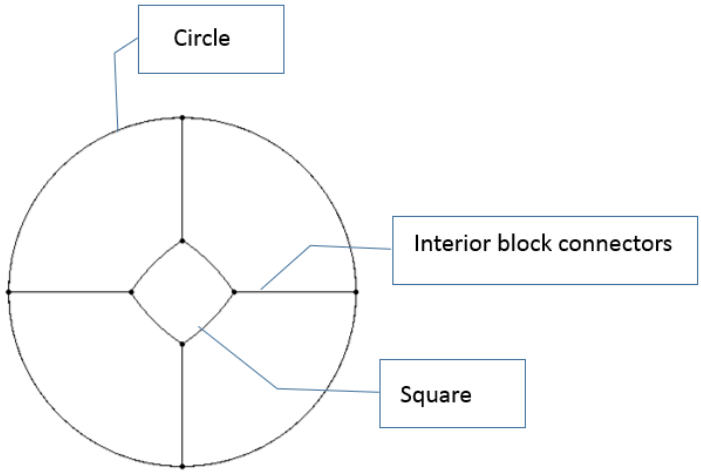

Figure 4 Grid Dimension on O-H Topology

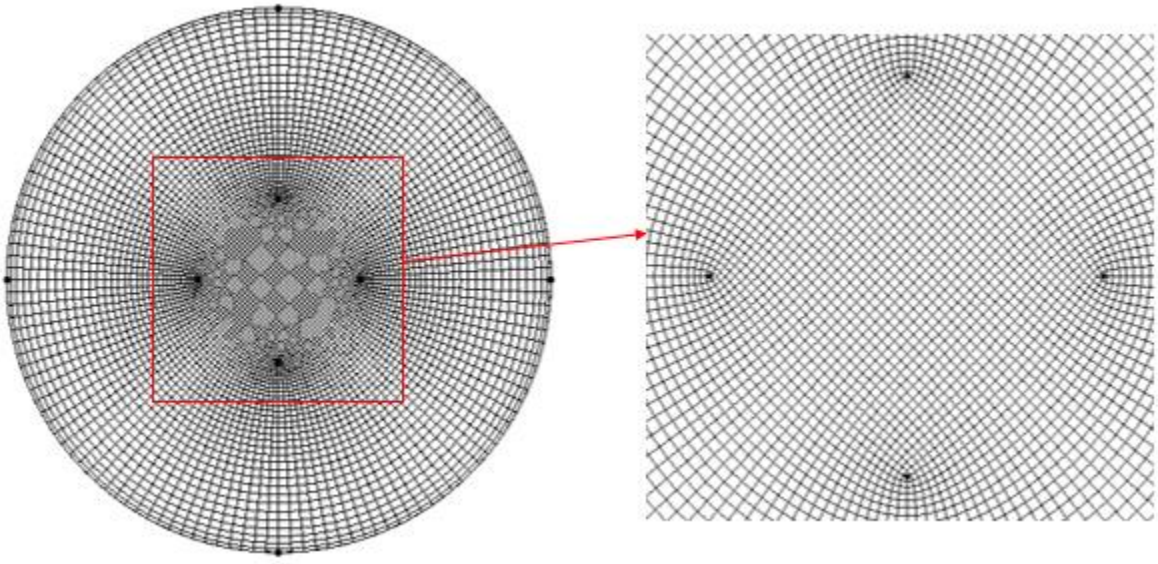

Figure 5 O-H Grid Topology on a cross-sectional plane

2.3 Numerical Method

.Numerical model involves the steady state solution of the governing equations of mass, momentum and energy in the computational domain. For an incompressible laminar flow in a helical tube, the simplified Navier stokes equations for conservation of mass, momentum and energy are solved

Continuity equation

$$\nabla.\vec{V} = 0 \qquad \text{Equation 4(a)}$$

Momentum equation

$$V.\nabla(\vec{V}) = \frac{-\nabla P}{\rho} + \frac{\mu\nabla^2\vec{V}}{\rho} \qquad \text{Equation 4(b)}$$

Energy Equation

$$\vec{V}.\nabla(T^*) - \frac{K\nabla^2(T^*)}{C_P\rho} = 0 \qquad \text{Equation 4(c)}$$

Where,

$\vec{V}$ = Velocity Vector

∇P= Pressure Drop

T^*= T-T_{wall}

μ=Dynamic viscosity

ρ=Denisty

C_P=Specific Heat

Ansys Fluent® 15.0 was used for all the numerical simulations in this study. Fluent uses finite volume method to solve the governing equations. Pressure based solver was chosen with coupled technique employed to handle the pressure-velocity coupling. Node-based approach is used to compute the gradients required for discretization of diffusive and convective fluxes. 2^{nd} order interpolation scheme is used for pressure and 2^{nd} order upwind discretization scheme is used for momentum equation. The convergence criterion of 10^{-6} was considered for residuals. The coupled AMG solver with Gauss-siedel method is used to solve the system of linear transport equations for pressure-based scheme. The average time taken to achieve the steady state solution on a 2.7GHz xeon Intel 16 core processor was 20mins.

The computational domain used in present study was on helical coil tube as described in previous section. Water at room temperature, was considered as a flowing fluid through the helical coil. At the inlet, a constant mass flow rate, flowing at a temperature (T^*) of 100K. Diameter of the tube (d) is taken as characteristic length used to calculate the Reynolds number. The outlet was set to pressure outlet boundary condition with gauge pressure equals to zero. No slip boundary condition was used for the wall boundary with wall temperature of (T_{wall}=0K).

2.4 Post-Processing

From the numerical results, the area weighted average values of temperature and pressure and heat fluxes data had been written to a file for post processing. Assessment of heat transfer performance of helical pipe is done by comparing the total heat transfer from the tube through the walls and pressure drop of the flow with that of fully developed flow in straight tube with same arc length (l) and cross-sectional tube diameter (d).

Temperature and Pressures were obtained from fluent and with that in hand, total heat transfer from the tube through the walls of a helical pipe and heat transfer enhancement are evaluated in Matlab using

$$\delta T^* = T^*_{in} - T^*_{out} \qquad \text{Equation 5}$$

$T^*_{in} = Inlet\ Temperature$, $T^*_{out} = Outlet\ temperature$ are the area weighted average values of temperature at inlet and outlet.

The ratio of Heat transfer to that of Power required to overcome the friction is calculated for helical coil tube is calculated as

$$\zeta_{helix} = \frac{\dot{m} C_p \delta T^*_{helix}}{\Delta P * Q} \qquad \text{Equation 6}$$

Heat transfer enhancement is defined as

$$\eta_{HT} = \left[\frac{\dot{m} C_p \delta T^*_{helix}}{\dot{m} C_p \delta T^*_{straight}} - 1 \right] \times 100 \qquad \text{Equation 7}$$

Relative pressure drop penalty going from straight to helix pipe is calculated by

$$\eta_f = \left[\frac{Pressure{-}drop_{helix}}{Pressure{-}drop_{straight}}\right] \quad \text{Equation 8}$$

Where

$\dot{m}$ = Mass flow rate = $\boldsymbol{\rho}$ UA

C_p= Specific heat of the water

A= Area of the cross-section.

U= velocity normal to the boundary.

Q= Volumetric Flow rate

$$Pressure - drop = \Delta P = Pressure_{outlet} - Pressure_{inlet}$$

Where δT^*_{helix} and $\delta T^*_{straight}$ are temperature difference between inlet and outlet boundary for helix and straight geometry respectively.

$Pressure_{inlet}$ and $Pressure_{outlet}$ are the area-weighted average pressure values at inlet and outlet.

CHAPTER 3 PARAMETRIC STUDY OF LAMINAR FLOW IN A HELICAL PIPE WITH CIRCULAR CROSS-SECTION

3.1 Data Set

Parametric study of heat transfer from helical coil tube through the wall was carried out by using laminar viscous model with water as flowing fluid. The parametric analysis have been carried out for Reynolds number from 35 to 500, Prandtl number Pr from 6.2 to 800, G3 from 2.3 to 9 and super-ellipse cross-sectional shape n from 2 to 9, for constant helical length and Pitch, G1=200 and G2=1 respectively. Full data set matrix was generated with 27 values of Reynolds number in the range 35 to 500, 3 values of Prandtl numbers (6.2, 400, 800), 7 values of G3 (2.3, 3.1, 3.9, 4.7, 6.3, 7.1, 9) and 8 different shapes are considered for the parametric analysis.

3.2 Results and Discussion

3.2.1 Mesh Generation and Grid Independence Study

Richardson Extrapolation was used for grid independence study. Richardson extrapolation is used to improve the rate of convergence of a sequence, from a higher order estimate from a series of lower order discrete values. For a Grid independence study, the value estimated from the Richardson extrapolation would result if the mesh size tend to zero. The level of grid convergence is estimated by using Grid Convergence index. Convergence study was conducted with 3 different mesh sizes for helical pipe with the grid refinement ratio r, as 1.3.

Helical pipe with geometric parameters G1=200,G2=1 and G3=9 with flow properties of Re 500 and Pr 6.2 is used for Grid Independence study and discretization was done using Pointwise grid generation tool. Grid Dimensions and Sizes are tabulated in table 1.

Mesh	Grid Dimension	Extrusion along helix axis	Grid size
Coarse	20 X 20	1500	~ 2.7 million
Medium	26 X 26	1950	~6.0 million
Fine	34 X 34	2500	~14 million

Table 1 Grid Dimensions and Size

The Generalized Richardson extrapolation was given by Roache [22] by introducing the p^{th} order method. The extrapolated value is varied by different choice of p order.

$$f_{exact} = f_1 + \left[\left(\frac{f_1 - f_2}{r^p - 1}\right)\right] \quad \text{Equation 9}$$

The order of accuracy can be found by

$$p = \frac{ln\left(\frac{\varepsilon_{32}}{\varepsilon_{21}}\right)}{\ln(r)} \quad \text{Equation 10}$$

$$\varepsilon_{i+1,j} = f_{i+1} - f_i \quad \text{Equation 11}$$

The convergence conditions are determined by using convergence ratio R,

1. Monotonic if 0<R<1

2. Oscillatory if R<0
3. Divergence R>1

Where,

$$R = \frac{\varepsilon_{21}}{\varepsilon_{32}}$$

For the Grid Independence study, the order of accuracy of outlet temperature was taken as a parameter. The convergence conditions of the simulation results are monotonic.

Roache [22] concluded that the GCI provides a measure of convergence for refinement studies, based on estimated fractional error derived Richardson extrapolation.

$$GCI_{i+1,j} = F_s \left(\frac{|\varepsilon_{i+1,j}|}{f_i(r^p - 1)} \right) \quad \text{Equation 12}$$

Factor of safety is considered as 1.25 for this study. Table [2] illustrates the Grid Convergence index for the study.

Grid	**Outlet Temperature (K)**	**GCI**
Fine – Grid 1	2.83988	$GCI_{12} = 0.003$
Medium – Grid 2	2.7998	$GCI_{23} = 0.01$
Coarse – Grid 3	1.88552	

Table 2 GCI for Grid Independence Study

There is a reduction for successive grid refinements ($GCI_{21} < GCI_{32}$) for the Outlet temperature. From the GCI values we can clearly see that the dependency of Numerical simulation on the Grid size has highly decreased for finer grid when compared coarser grid. The grid independent solution suggests that further refinement on grid after the finer grid doesn't affect the simulation results, so finer grid is selected for further study.

3.2.2 Validation of Numerical Solver

Validation of Numerical method was done by comparing the published work by Pawar [7] in IChemE. The computational model used for validating the numerical solver was same as that of experimental setup and CFD model used for conducting convective heat transfer in helically coiled tube heat exchanger by Pawar. The helically coiled tube have the Tube to coil diameter as 0.0757. Shell conduction model in Fluent was used to model the wall thickness of 2.3mm for which meshing of wall thickness is not necessary. Convective heat transfer in the vessel maintained at 62.5^{o}C. Inner and outer walls are coupled for energy transfer from hot fluid inside the vessel to cold fluid through the coil. Coil material used for shell model is mild steel with thermal conductivity of 52(W/m-K), Specific heat 620 J/Kg-K and density 7850 Kg/m^3. Inlet was taken as Mass flow inlet boundary condition and hot fluid at outlet of coil was specified as pressure outlet at zero back pressure. Laminar incompressible Navier Stokes governing equations are solved in fluent using SIMPLE algorithm with second order accuracy with

relative convergence criterion of 1e-5 for continuity, X,Y,Z velocities and energy equation. Outlet temperature based on area-weighted average was compared at 2 different Reynolds number.

Typical Boundary conditions used for the validation case are tabulated in Table

Inlet temp (^oC)	Reynolds number	Mass Flow rate (Kg/s)	h_o (W/m^2-K)
32	4321	0.04148	926
37.5	7098	0.06811	907.68

Table 3 Boundary conditions for validation case

Re	Experimental (REF)	Simulation (REF)	Simulation
4321	59	57	57.314
7098	56	54.5	55.176

Table 4 Comparison of Outlet Temperature

It can be seen from the comparison of outlet temperatures (^oc) of water flowing through the helical pipe that results from the numerical solver shows good agreement with the experimental data and Numerical results as published.

3.2.3 Baseline Geometry

3.2.3.1 Flow Characteristics

Inside a Helical pipe, flow analysis shows, the pressure gradient is directed towards the center of the pipe cross-section to poise the centrifugal force generated due to curvature. Due to the circulatory motion of the pipe, fluid in the center region moves outwards, top and bottom fluid moves inwards in a given cross-sectional plane. Thus in a helical tube, adjustment of high velocity region towards the outer wall and thicker layer of slow moving fluid goes to the inner wall takes place. Magnitude of centrifugal force is known to be proportional to $\frac{v^2}{2R}$. To have centrifugal force balance, the pressure gradient is developed across the cross-section of the tube.

In any given cross-section, due to viscous effects, low velocities are present in boundary layer, while circumferential and rotational velocities has the same characteristics. Small centrifugal force is generated due to the low velocity in the boundary layer compared to the center region of the cross-section. Meanwhile pressure gradient is formed from outside to the center of the cross-section. Thus, this small centrifugal force and pressure gradient pushes the fluid from outer side to inner side for conservation of the mass. Along the mid-plane, the flow has high velocity and has high centrifugal force, thus yielding in moving the fluid to outer boundary from the inner side. Due to this movement of fluid from one side of the boundary to another, secondary flow is formed in the cross-section to have 2

symmetric circulating flow. For low Dean number secondary low streamlines are symmetric and convex. While the Dean number is increased the intensity of secondary flow increased causing the non-convex regions are developed by forming dimples in the streamlines of the secondary flow. The Secondary flow streamlines for Dean number 23.08, 170.77 and 329.7 for a given curvature ratio G3 = 2.3 are shown in Figure 6. For low Dean number's the streamlines are symmetric as shown in Figure 6. Streamlines shows that the secondary flow takes much greater values on the inside of the cross-section.

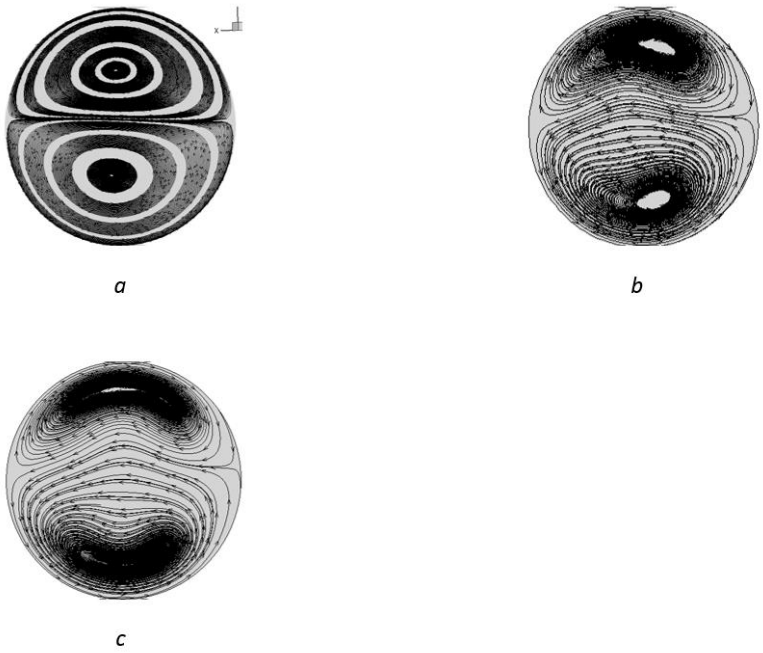

Figure 6. Streamlines at Dean number (a) De=23.08 (b) De= 170.77, (c) De= 329.7

Temperature contours taken at mid-section of total length in a helical pipe with varying G3 are shown in Figure 7. Symmetric behavior along top and bottom side

of the helical tube cross-section is due the effect of secondary motion. As the coil to tube diameter is increasing the temperature distribution increased.

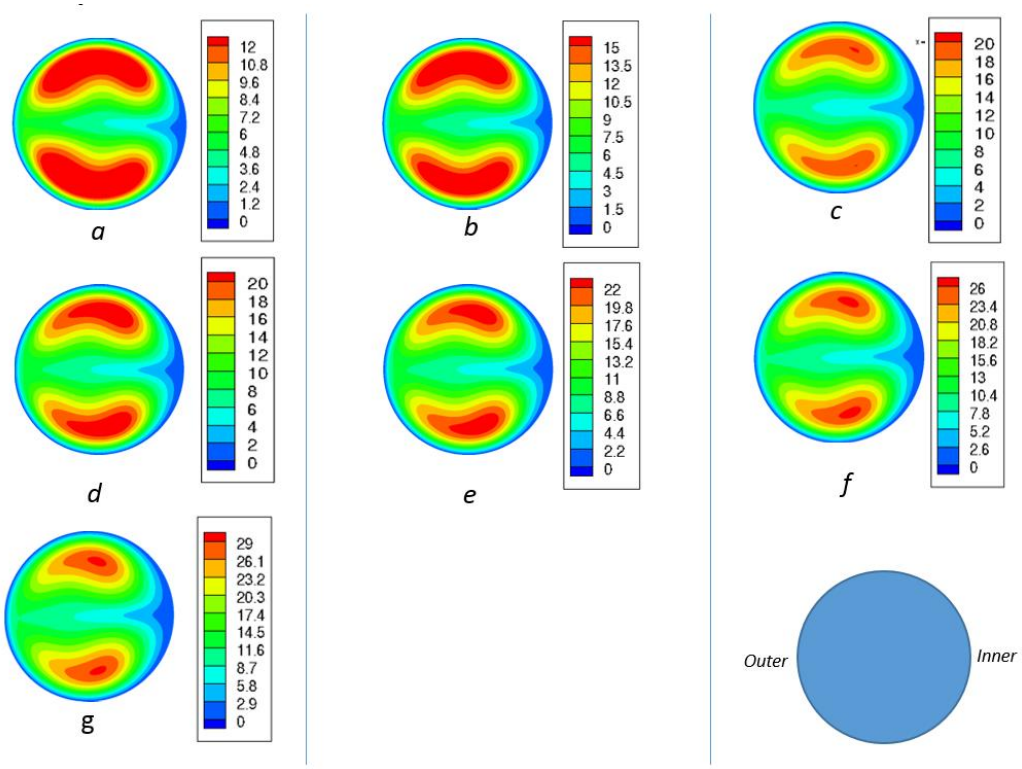

Figure 7 Temperature contours at taken at 50% length at Dean number: (a) De=329.7;(b) De=283.98;(c) De=253.1848;(d) De=230.6328;(e) De=199.2048;(f) De=187.6467;(g) De=166.67

The temperature distribution in a helical pipe with Dean number 329.7 along the plane AA and BB at different lengths are plotted in Figure 8. There are some oscillations in the temperature distribution along the plane AA, due to the secondary flow. A symmetric temperature distribution is found along plane BB, which concludes there is a secondary flow vortices called Dean Vortices present in a given cross-section of helical pipe.

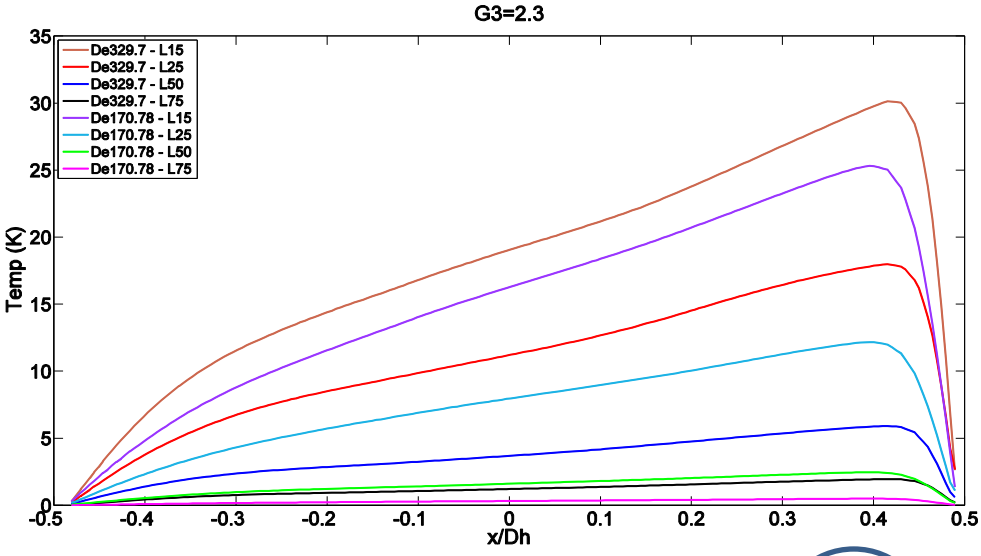

(a)

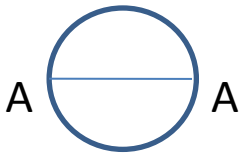

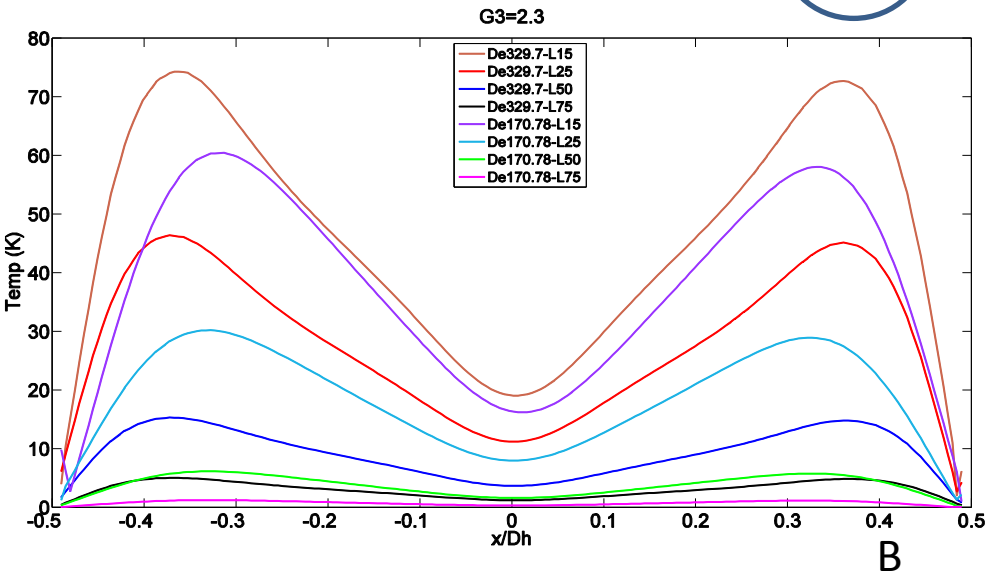

(b)

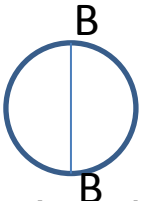

Figure 8Temperature Distribution for De 329.7 at Different lengths a) along plane AA b) along Plane BB

In order to demonstrate the effects of helical non-dimensional parameters on heat transfer when compared with that of a straight tube, the heat transfer enhancement and pressure drop parameters are determined using Equations 6 and 7. These parameters show the advantage of helical coil's over straight tube and also the effect of helical coil over each other. For comparison with a straight tube, analysis was conducted on a baseline geometry-1, straight tube with diameter (d) and G2 =200, with same range of Re and Pr numbers

3.2.3.2 Effect of Reynolds number

As the Reynolds number increases, centrifugal force induced in the flow also increases, which in turn increases the heat transfer from the tube to the wall.

Ratio of heat transfer to power required vs Reynolds number for given coil to tube diameter 2.3, shown in Figure 9. At low Reynolds numbers, ζ_{helix} decreases rapidly till Re 150 and then decreases tardily and remains almost constant at higher Reynolds number.

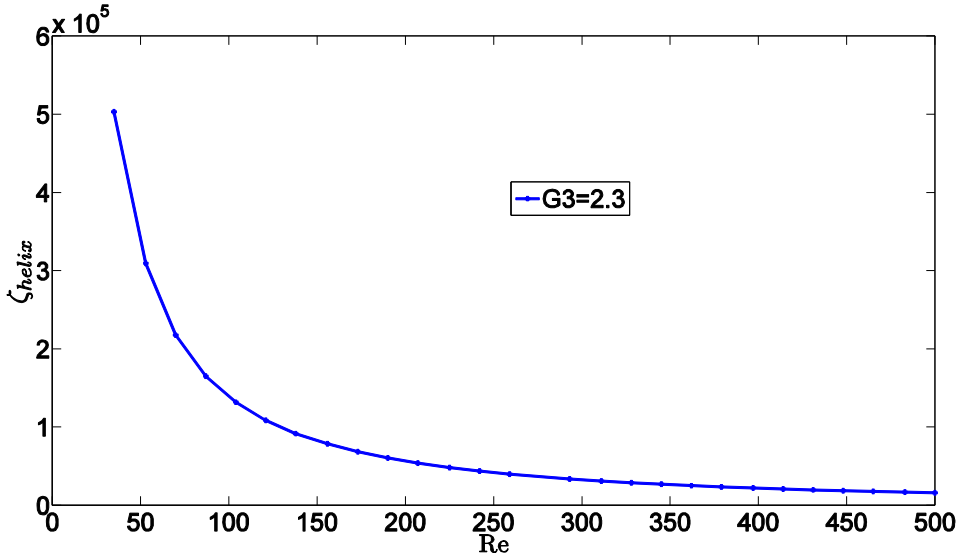

Figure 9 ζ_{helix} vs Re for G3 = 2.3

Figure 10 and 11 illustrates the heat transfer enhancement and pressure drop over a range of Reynolds Number and for a given curvature ratio of G3=2.3 with water as flowing fluid with a Prandtl number of 6.2. As the Reynolds number increases the Heat transfer enhancement gradually increases. At low Reynolds numbers there is no significant enhancement in Heat transfer. As the Reynolds number increases the pressure gradient increases which can be seen in Figure 9. The power required to overcome the friction of the flow increases with increase in Reynolds number. Helical coil requires more power than the straight tube to overcome the effects of secondary flow.

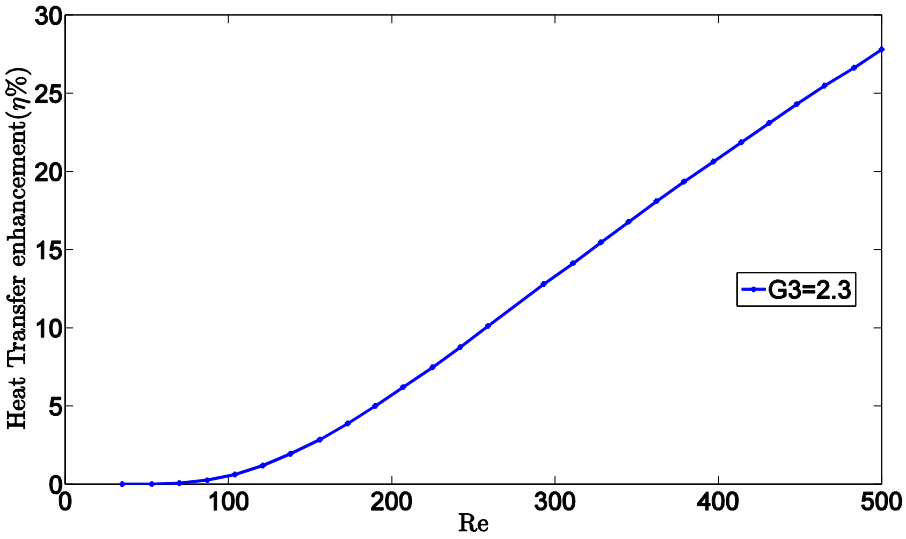

Figure 10 Heat transfer enhancement for G3=2.3

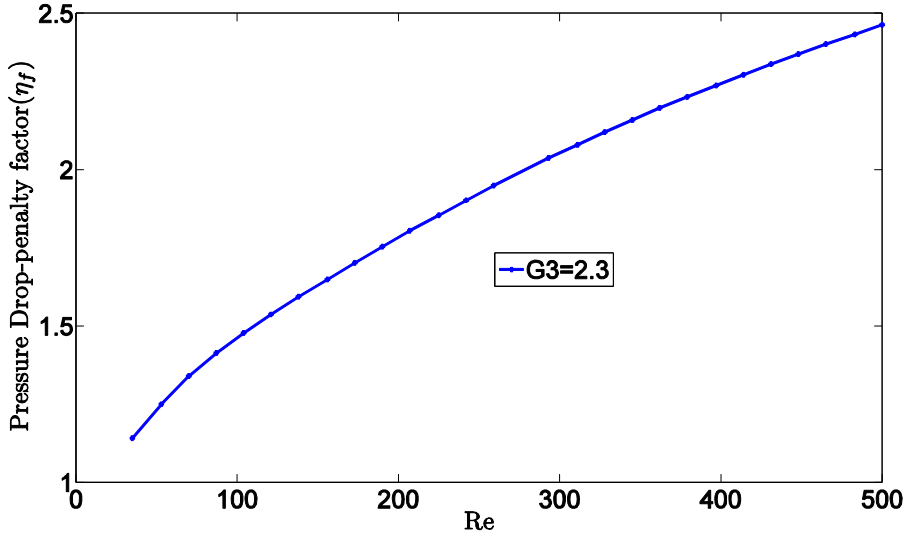

Figure 11 Pressure Drop enhancement for G3=2.3

3.2.3.3 Effect of Prandtl number

For low Prandtl numbers the maximum temperature occurs near the diameter of the symmetry. Temperature contours for Prandtl number 6.2 Figure 8 are skewed

towards the outer wall. The temperature contour for Dean number 378.9 at 3 different Prandtl numbers are shown in Figure 12.

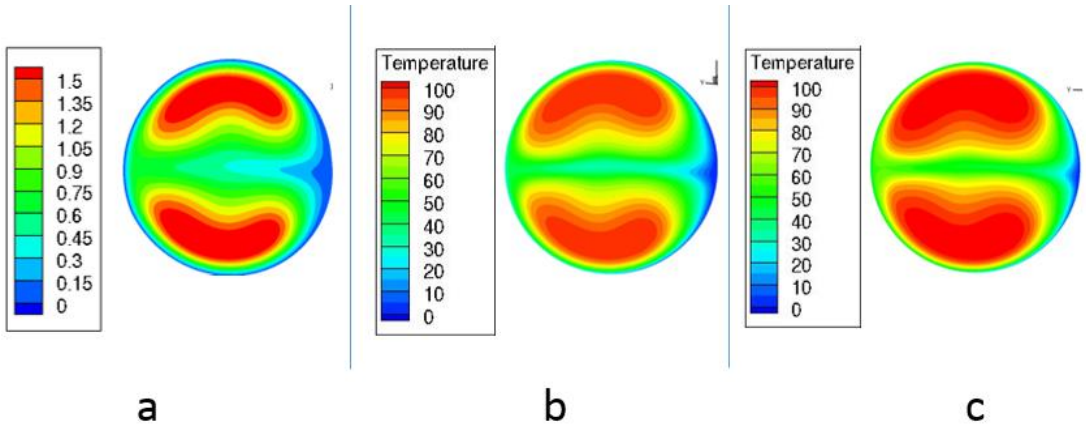

Figure 12 Temperature contours for De 329.7 a) Pr=6.2, b) Pr=400, c) Pr=800

Prandtl number is a dimensionless number defined as ratio of momentum diffusivity to thermal diffusivity. From the analysis it was observed that, as the Prandtl number increases the effect of convective terms also increases for a given G3. Ratio of Heat transfer to power required for constant G3 of 2.3 is plotted for different Re in Figure 13. It is observed that ζ_{helix} decreases as Prandtl number increases for a given G3. At high Reynolds numbers, ζ_{helix} is constant for Prandtl number 400 and 800.

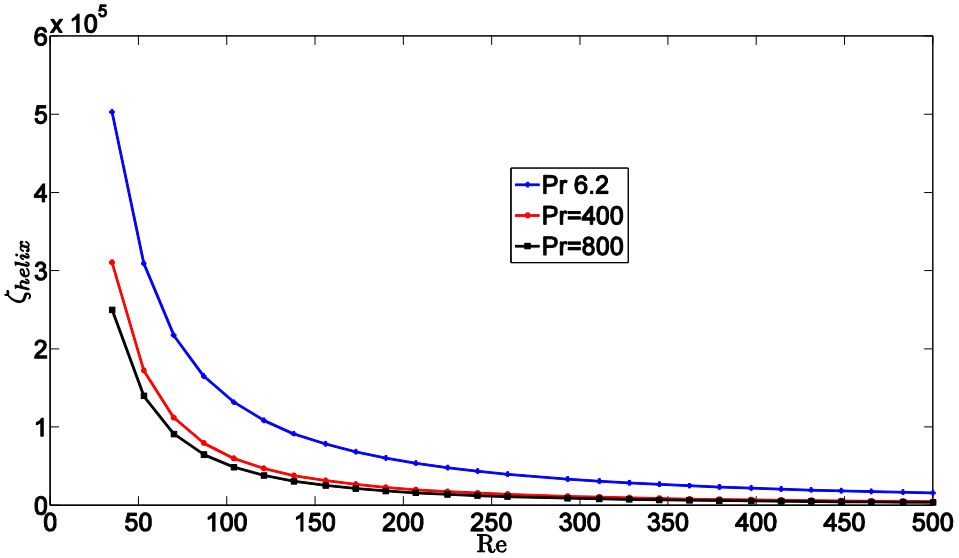

Figure 13 Ratio of Heat transfer to Power required for different Prandtl number for G3=2.3

The heat transfer enhancement and pressure drop friction factor when compared with straight tube are plotted in Figure 14 and 15 for different Prandtl numbers 6.2, 400 and 800. It is clearly seen that the Heat transfer enhancement increases as Prandtl number increases for constant G3 2.3. Sudden rise in Heat transfer is observed at low Reynolds number less than 100. For Prandtl number 800 there is a less enhancement in heat transfer than Prandtl number 400 at high Reynolds numbers. There is a constant enhancement in pressure Drop as Prandtl number increases. Power required to overcome the friction remains constant even if Prandtl number increases flowing at a constant volumetric flow rate.

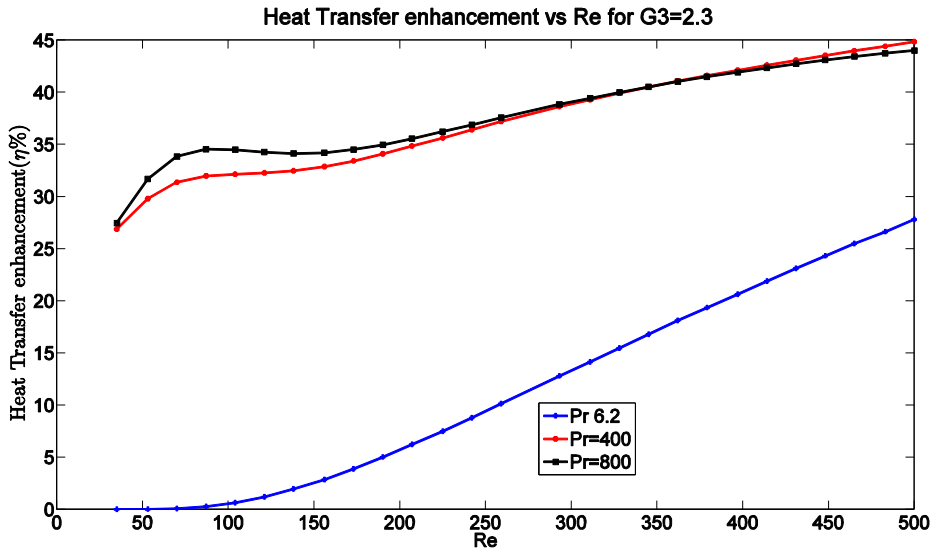

Figure 14 Heat transfer enhancement for G3 = 2.3

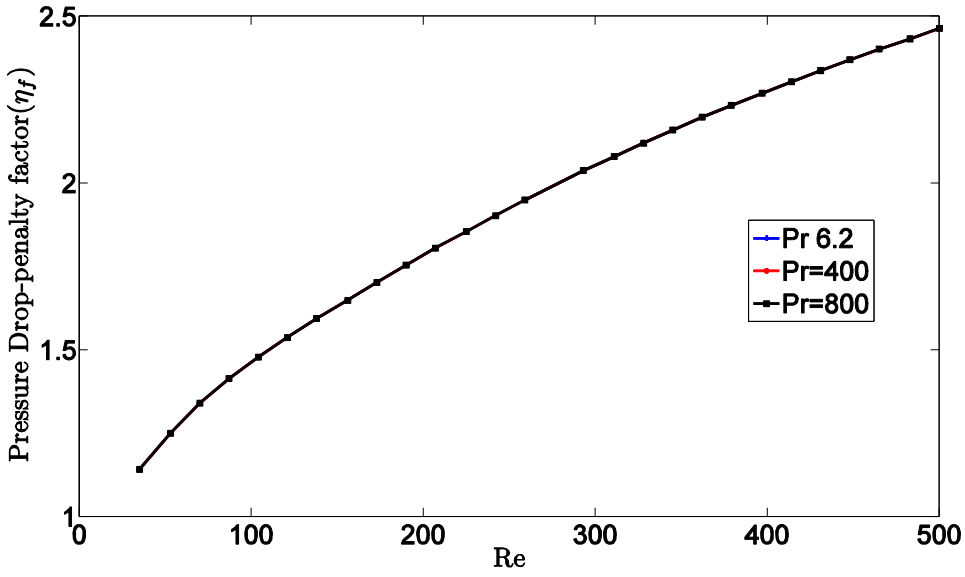

Figure 15 Pressure drop enhancement for G3 = 2.3

3.2.3.4 Effect of Helical Coil Diameter

Coil diameter influences the centrifugal force on the fluid which in-turn effect the secondary flow along the helical pipe. As the curvature of the helical pipe increases, the effect of centrifugal forces plays a lesser role in the flow characteristics. Ratio of Heat transfer to Power required for different G3's are plotted for range of Reynolds numbers in Figure 16 and Figure 17. It is observed that as G3 increases the Ratio of Heat transfer to Power required increases at low Reynolds number's and remains constant at high Reynolds numbers.

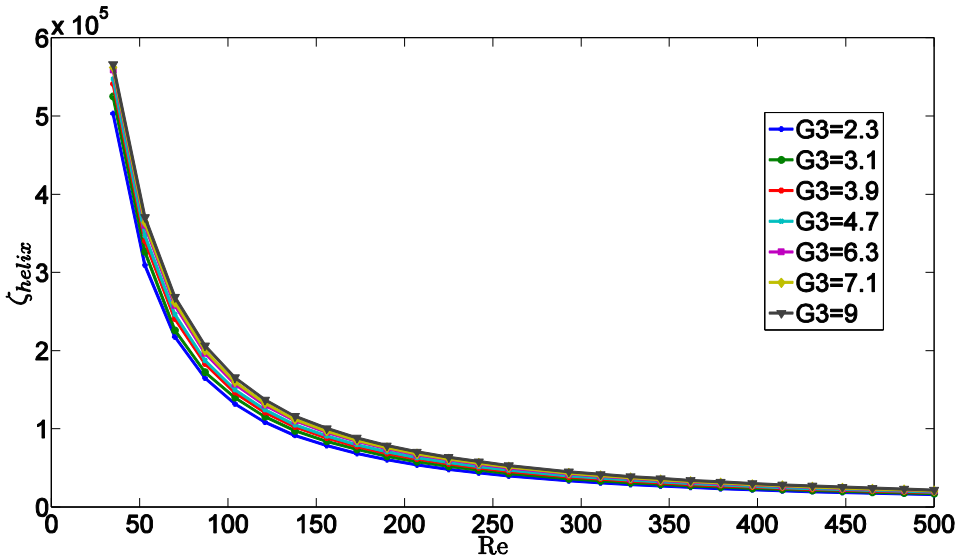

Figure 16 ζ_{helix} vs Re for different G3

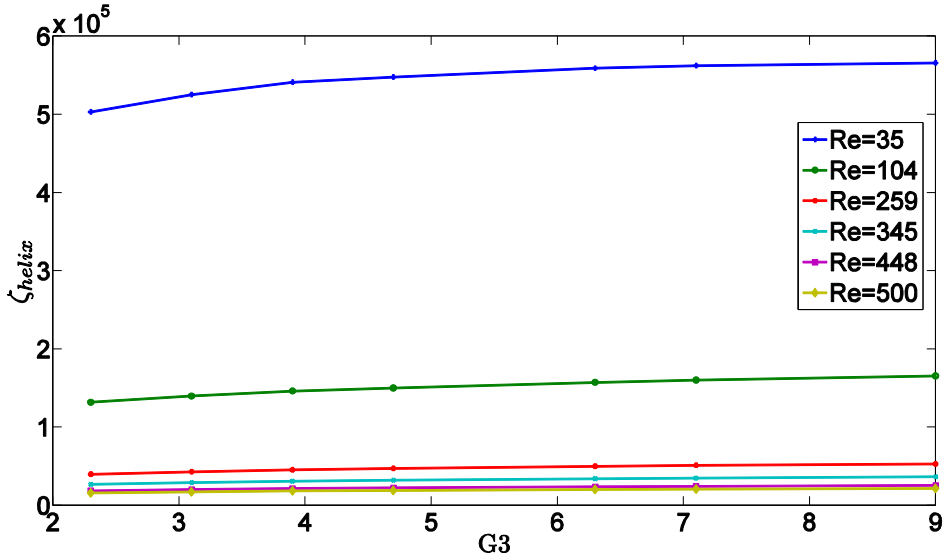

Figure 17 ζ_{helix} vs G3 for different Re

The effect of G3 on heat transfer enhancement vs Reynolds number is plotted in Figure 18. As the G3 increases the Heat transfer enhancement is decreased for a constant Reynolds number. Up to Reynolds number 250 there is no significant enhancement in the heat transfer by changing the G3. Above Reynolds number 250, enhancement in the heat transfer decreases with increase in G3 as shown in Figure 19.

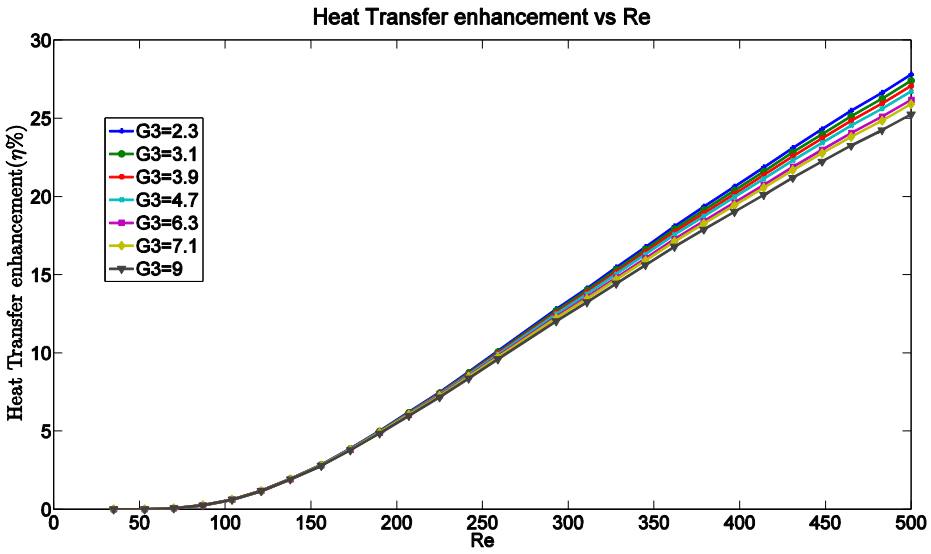

Figure 18 Heat transfer enhancement for Different G3

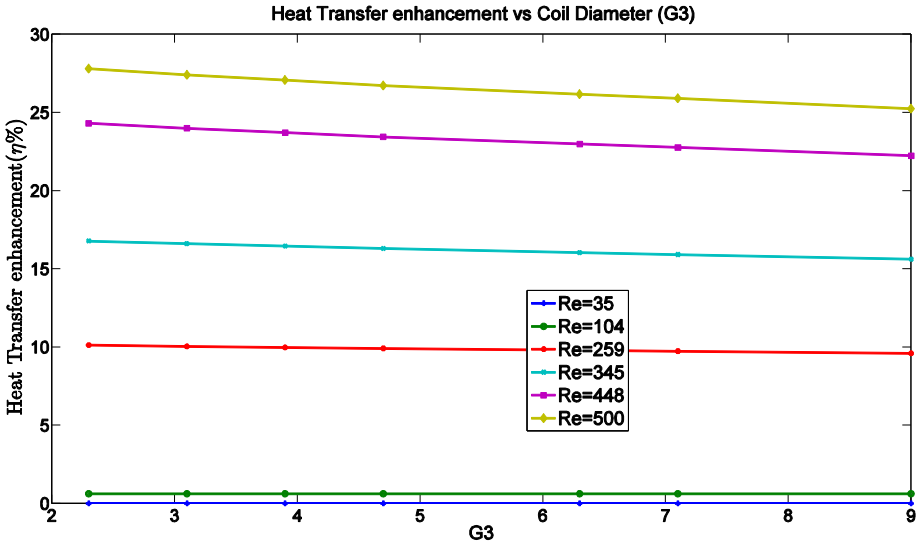

Figure 19 Heat transfer enhancement vs G3 for different Re

As the curvature increases the pressure gradient decreases along the pipe due to decrease in intensity of secondary flow. The pressure drop enhancement decreases as the G3 increases.

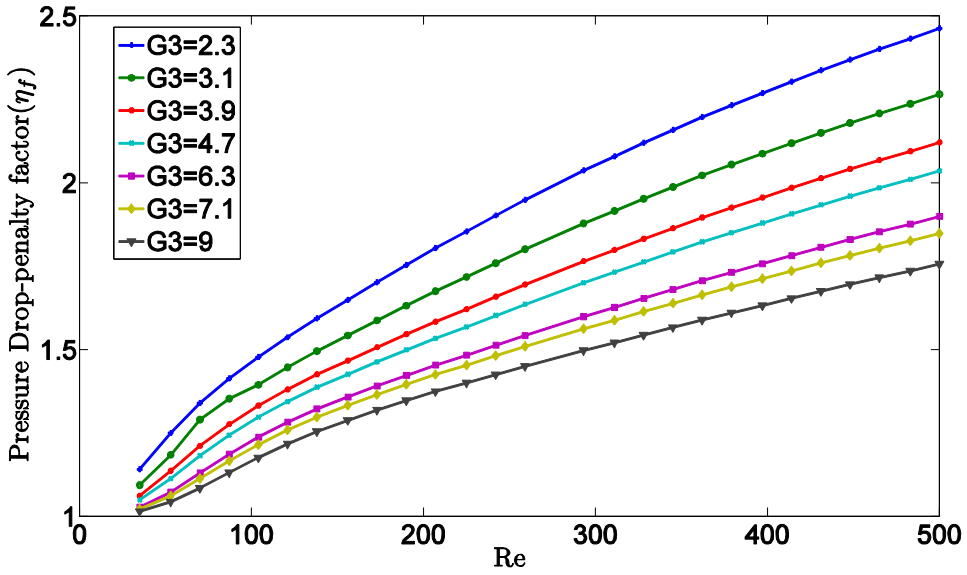

Figure 20 Pressure drop enhancement vs Re for different G3

3.2.3.5 Effect of Shape Power Factor (n):

The cross-sectional shape was varied in the range of n=2 to 9, with geometric parameters and flow parameters as K_{ab} =1, G3=2.3,G3=30, G2=1, Re 500 and Pr=6.2. Ratio of Heat transfer to power required is plotted in Figure 21 for different cross-sectional shapes with constant hydraulic diameter of 0.5mm.It was observed that ζ_{helix} increases as power factor (n) of super-ellipse equation increases.

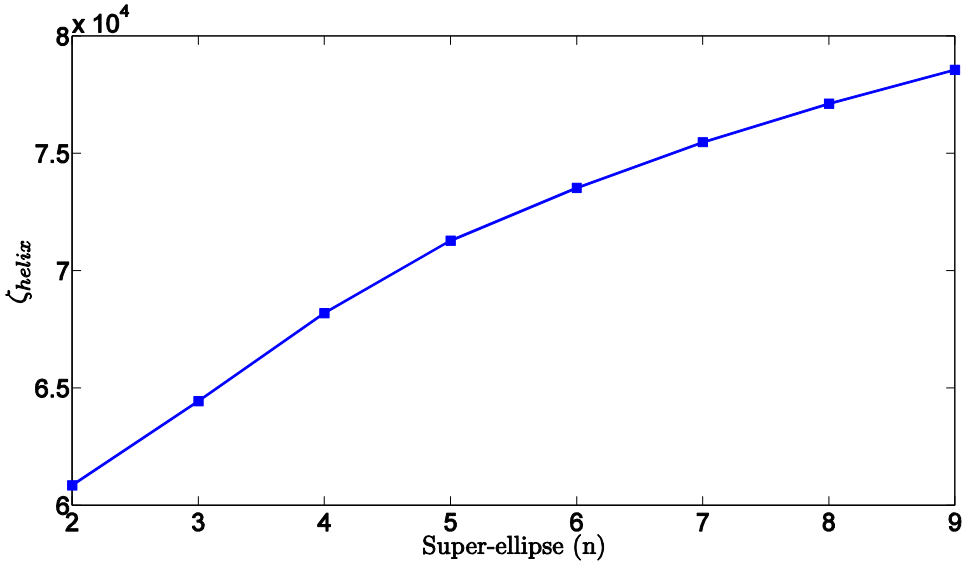

Figure 21 Ratio of Heat transfer to Power required for different cross-sectional shape.

The effect of 'n' on heat transfer and pressure drop when compared with straight tube are plotted in Figure 22 and 23. It is observed that, the heat transfer enhancement and pressure drop are sensitive to the cross-sectional shape. As n increases, heat transfer enhancement decreases. The maximum enhancement 38.71% in the heat transfer can be seen at n=2 and with a minimum of 31% is seen for n=9 when compared to straight tube. As n increases the pressure drop enhancement decreases. Power required to overcome the friction is directly proportional to pressure drop as shown in equation 12.

$$Power = \Delta P * Q \qquad \text{Equation 13}$$

Where,

$$\Delta P = pressure\ drop$$

$$Q = volumeteric\ flow\ rate$$

As n increases the power required to overcome the friction decreases .i.e power required for the flow to overcome the effect of secondary flow is sensitive to the shape of the tube cross-section.

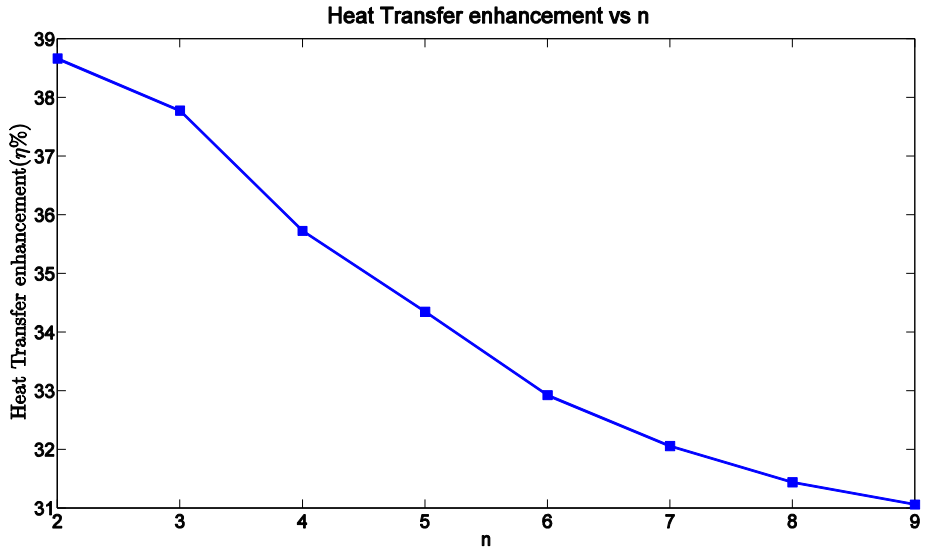

Figure 22 Heat transfer enhancement vs n

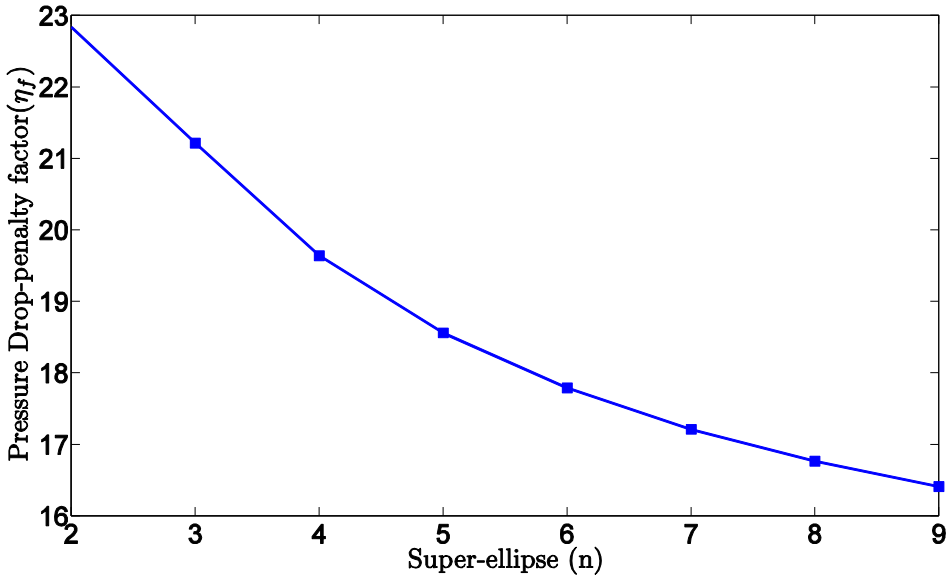

Figure 23 Pressure drop enhancement vs n

Conclusion

A comprehensive parametric study involving a complete set of non-dimensional parameters has been performed for laminar flow using computational fluid dynamics. The non-dimensional parameters governing the flow through the helical tube are the Re from 35 to 500, Pr of 6.2, 400 and 800, G3 from 2.3 to 9, G2=1, G1=200 and n from 2 to 9. The overall effect of these non-dimensional parameters on heat transfer from the tube through the wall and pressure drop when compared to straight tube are presented. The parametric analysis shows that, as Reynolds number increases the heat transfer and pressure drop enhancements increases for a given G3. At low Reynolds numbers there is no significant enhancement in Heat transfer. Heat transfer enhancement increases as Prandtl number increases. For high Prandtl numbers, there is a local peak of heat transfer enhancement at low Reynolds number. At high Reynolds numbers in laminar region, Pr 800 shows lesser heat transfer enhancement as compared with Pr400 for a given G3=2.3. This study also shows that, as G3 increases, intensity of secondary flow in the helical pipe is decreased. This decrease in intensity of secondary flow reduces the heat transfer from the tube through the walls. For low Re, the heat transfer enhancement is almost constant and a significant decrease in heat transfer enhancement is observed only at higher Reynolds number. From the parametric analysis conducted with varying ‘n’, shows that the heat transfer enhancement and pressure drop of a helical coil is sensitive to the cross-sectional

shape of the helical coil. For non-dimensional parameters G3=2.3, G1=30, G2=1, Re 500 and Pr of 6.2, the super-ellipse cross-sectional shape with shape power factor n=2 has a maximum enhancement in heat transfer and Pressure drop decreases with increase in n. From the parametric analysis, it can be concluded that, to achieve high Heat transfer enhancement from the tube through the wall, a smaller G3, larger G1, Re and Pr is desired and also it is sensitive to the non-dimensional parameters G2 and n.

CHAPTER 4 SHAPE OPTIMIZATION OF A HELICAL TUBE

The purpose of this chapter is to demonstrate a fully automated process for optimizing the shape of a helical coil tube and maximize the total heat transfer from the tube through walls while enforcing the constant hydraulic diameter for the cross-sectional shape. The design system required to maximize the heat transfer incorporated the automated mesh generation with computational fluid dynamics solver. The flexibility and automation of the design systems allows it to easily integrate with other programs to optimize the helical tube for maximum heat transfer from the tube through the walls.

4.1 Optimization Computing Toolbox

4.1.1 Methodology

Automated and straightforward design framework is required to achieve the objective of the current study. Interaction and integration of different physical systems, such as Grid generation pre-processor, analyze and optimize the design space, to achieve an objective or multi-objectives, requires quite a few programs and files with user inputs. A simple automated optimization methodology was implemented in this study. Modular system steered to ease the communication between user and computer, by simplifying the design process. A modular system can be characterized by functional skids or modules which can be replaced or removed without effecting the flow process. Figure 24, illustrates the concepts of modular system used in this study, which apply to the optimization of helical coil

tube. The optimization modular system is divided into 4 different sub-systems, first being the preprocessor module which generates the grid using user input geometric parameters for computational domain and exports the output as a specific file for the numerical solver module. Numerical solver module solves the Governing equations and outputs the information to the post processing module. The post-processing module calculates the objective function and passes it to the optimizer. Optimizer runs in loop until it finds the maximum of the objective function. Details of each sub-module are described in following sections.

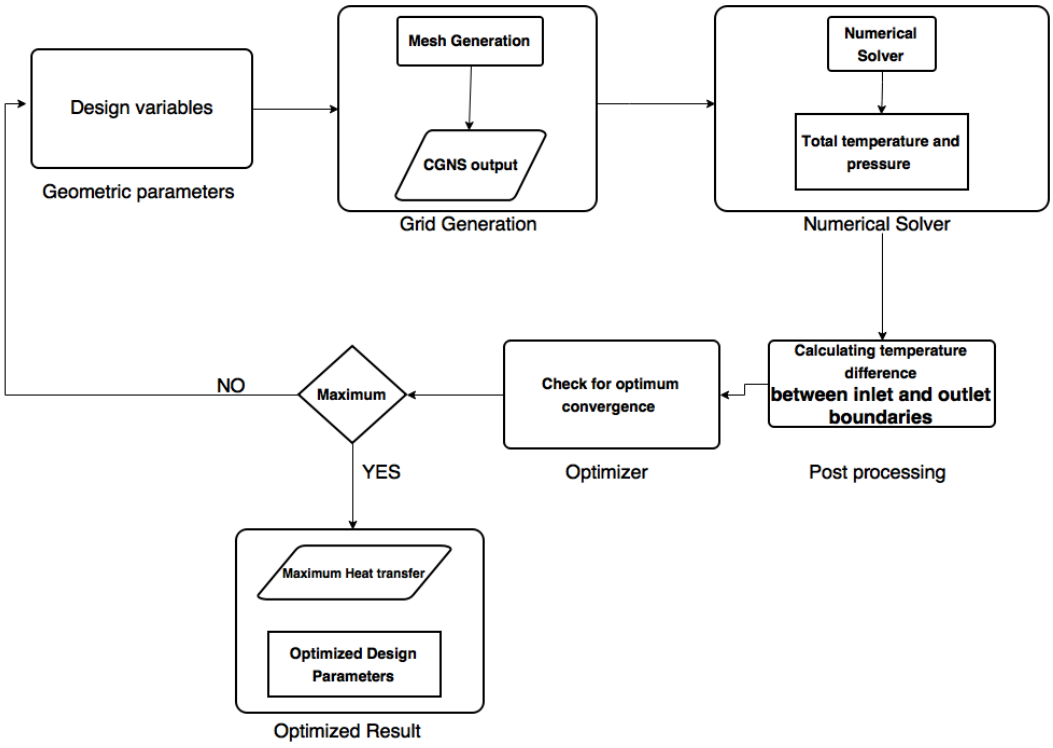

Figure 24 Flow chart of Modular system's used to Automate Optimization Process

4.1.2 Geometry Definition

The objective of the study was to find an optimum design of a helical coil tube to maximize heat transfer from the tube through the wall that enhances the efficiency of the helical tube. From the parametric analysis it was found that the heat transfer is sensitive to coil radius, pitch and the cross-sectional shape of the helical coil. Geometry of helical coil definition is described in section 2.1. To reduce the computational time the length of the helical tube was reduced to 15% of the total length used in parametric study. To optimize the helical tube 4 design variables K_{ab}, K_c, K_p and n were chosen which are sensitive to the objective function.

These design variables are set as a user input for the grid generation modular process.

4.1.3 Grid Generation

Altair HyperMesh V14.0 was used to generate the grids for this study. The computational domain was discretized with structural elements. As the structural domain and grid dimensions from the Grid independence study conducted for the parametric analysis are taken for the optimization study. As the total length considered for this optimization is reduced, number of steps used in extrusions are reduced. The scripting capabilities of HyperMesh were used to discretize the computational domain and which can be easily integrated into the optimization process. The automated script generates the grid based on the user defined helical geometric parameters such as radius of major and minor axis of the tube cross-

section, Coil radius, pitch and length. Hydraulic Diameter of the tube cross-section is maintained as that of circular cross-section. The automated script sets up the inlet boundary condition for the helical coil and exports the file as an input for the Solver.

4.1.4 Numerical Solver

4.1.4.1 Computational Domain and Boundary Conditions

The output file from grid generation process was used as input to the numerical solver. The governing equations of fluid flow are solved using the numerical method as described in section 2.3. Once the input is imported into Ansys fluent, UDF was used to identify the outlet boundary and pressure-outlet boundary is applied to it. Mass flow inlet and no-slip boundary condition was applied at inlet and wall.

4.1.5 Post-Processing

Once the solution converges, the solver writes all the required data in a file, i.e. Area averaged values of temperature and pressure. A script was passed through the Matlab modular system which calculates the δT and send the information to the optimizer module.

4.1.6 Optimization

In order to maximize the heat transfer from the tube through the walls in a helical coil tube defined by the design parameters in section 4.1.2, a simple and robust optimization algorithm was chosen. The process of finding a minimum or

maximum value of a function while varying the parameters subjected to any constraints is called optimization. The goal of the optimization algorithm is to find a maximum of temperature difference between the inlet and the outlet boundary condition (δT) more efficiently in the given range of design parameters, Matlab's inbuilt constrained non-linear convex optimization algorithm "active-set" was chosen for this study. Finding a global maxima is out of scope of this study.

Matlab Optimization Tool Box: Choosing the Algorithm

Matlab's FMINCON optimization tool box have different algorithm options like Interior-point, trust-reflective-region, SQP, Active-set. From the previous study conducted for Size Optimization of RACE CAR Chassis structure gave an insight and advantageous of using active-set algorithm. Table 5 below shows the Optimized Design variables subjected to minimizing the weight of the Chassis structure.

It was observed that there was a maximum of 3% error in Design variables and the objective function with different algorithms. Active-set algorithm was seen more effective in finding the optimum with less time than other algorithms used Problem definition reported in Appendix B

Optimized Design Variables (mm)			Weight		
Active Set	Interior-Point	SQP	Active Set	Interior-Point	SQP
1.91	2.1	1.91	27.655	28.285	27.475
13	13	12.7			
1.91	2.3	1.91			
14	14	13.32			
1.55	1.65	1.55			
13	13	12.7			

Table 5 Optimized Result for RACE CAR Chassis Structure using Fmincon with different algorithm

4.1.6.1 FMINCON Active Set Algorithm

Matlab's Fmincon is a non-linear convex optimization with Active set algorithm, which is designed to find a minimum or maximum of an objective function f(x) based on linear and non-linear constraints by solving Karush-Kuhn-Tucker equations and used quasi-newton method to approximate the hessian matrix.

4.1.7 Optimization Problem Statement

1. Objective Function: Maximize the temperature difference between the inlet and the outlet boundary condition are maximized (δT^*).

$$objective\ function = -\delta T^* \quad \text{Equation 14}$$

2. Design variables : 4 geometric parameters are used as design variables for optimization

$$K_{ab} = \frac{radius\ of\ cross{-}sectional\ Major\ axis}{radius\ of\ cross{-}sectional\ Minor\ axis} = \frac{A}{B} \quad \text{Equation 15}$$

$$K_c = \frac{Coil\ Diameter}{Major\ axis\ diameter} = \frac{D_{coil}}{2A} \quad \text{Equation 16}$$

$$K_P = \frac{Pitch}{Minor\ axis\ diameter} = \frac{P}{2B} \quad \text{Equation 17}$$

$$n = shape\ power\ factor\ in\ super - ellipse\ equation \quad \text{Equation 18}$$

3. Constraints: Upper bound and lower bound are set to the design variables, so that the design variables are always in the range.

Design variables	Lower Bound	Upper bound
K_{AB}	1	2
K_C	2.3	10
K_P	1	3
n	1.5	9

Table 6 Design variables for Optimization

4.1.8 Result and Discussion

From the parametric analysis it is found that the heat transfer from a helical coil tube through the wall is sensitive to Reynolds number, Prandtl number, coil diameter, length, pitch and cross-sectional shape of the helical coil. The baseline geometry was finalized with G3=2.3, G2=1 and G1 =30 with circular cross-section and used as initial guess for the optimization. Re 500 and Pr 6.2 are chosen as flow properties.

The Design variables used for shape optimization are K_{ab}, K_c, K_p and n. The upper bound and lower bound for these variables are considered for optimization and are tabulated in Table 6 and hydraulic diameter of the cross-section was maintained as that of baseline geometry. The optimization was done to maximize the temperature difference between the inlet and outlet boundaries(δT^*), which is directly proportional to the heat transfer from the tube through the wall. The optimization iteration output is documented in Appendix A. The Optimization run 1 finds the maximum heat transfer in 8 iterations with inner loop convergence simulations of 54. For Optimization run2, optimization took 5 iterations with lesser inner loop simulations of 45. The optimized cross-sectional shape with the initial guess obtained from parametric analysis is tabulated in Table 7.

Design Variables	**Initial Guess**	**Optimized variable**	δ**T* (K)**	$\dot{m}$**Cp** δ**T*** **(Js^{-1})**
K_{ab}	1	2	64.2507	47.0106
K_c	2.3	2.3017		
K_p	1	3		
n	2	2.6438		

Table 7 Optimization Result for Run1

As Matlab fmincon finds the local minima or maxima depending on the initial guess. Another run was done with different initial guess to find whether the optimized values are converging to a global point. Table 8 shows the optimization Run2 with different initial guess as that of Run1,

Design Variables	**Initial Guess**	**Optimized variable**	δ**T*** **(K)**	$\dot{m}$**Cp** δ**T*** **(Js^{-1})**
K_{ab}	2	2	64.2436	47.005
K_c	2.3	2.3116		
K_p	1.5	3		
n	1.5	2.4964		

Table 8 Optimization Result for Run2

The maximum error percentile between the optimized variables from 2 runs is found to be less than 5% leading to a global optimized variable. The enhancement of 37.35% is obtained with optimized shape when compared with straight tube

with same optimized cross-sectional shape. 45.85% increment with straight tube with circular cross-section and 5% of enhancement when compared with helical coil tube with circular cross-section of initial guess.

Super ellipse Shape	Heat Transfer ($\dot{m}$Cp δT) (Js^{-1})
Optimized Helix	47.0106
Helix –Circular Cross-section	44.8664
Straight-Optimized Cross-section	34.2263
Straight - Circular Cross-section	32.23

Table 9 comparison of Optimized Helical with cross-sectional shape.

Temperature contours of optimized shape, helical and straight tube with circular cross-section are plotted at 95% of G1 used for optimization are shown in Figure 25 Symmetric behavior along top and bottom side of the helical tube is due the effect of secondary motion.

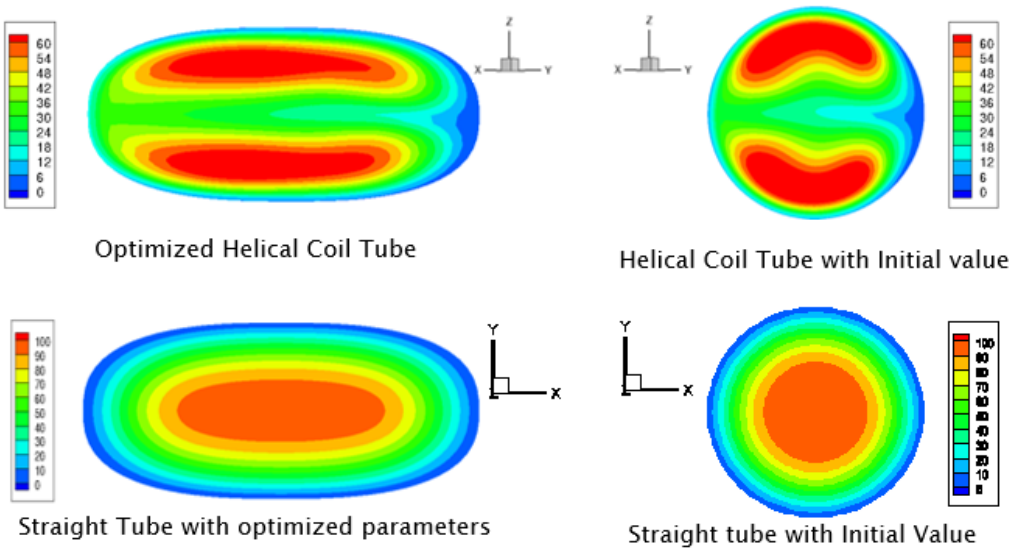

Figure 25 Temperature contours

The temperature distribution and helicity are plotted along plane BB at 95% of G1 used for optimization for optimized shape, helical tube with circular cross-section and straight tube with optimized cross-section. The symmetric behavior of temperature distribution and helicity shows that the symmetric vortices are present in the cross-section.

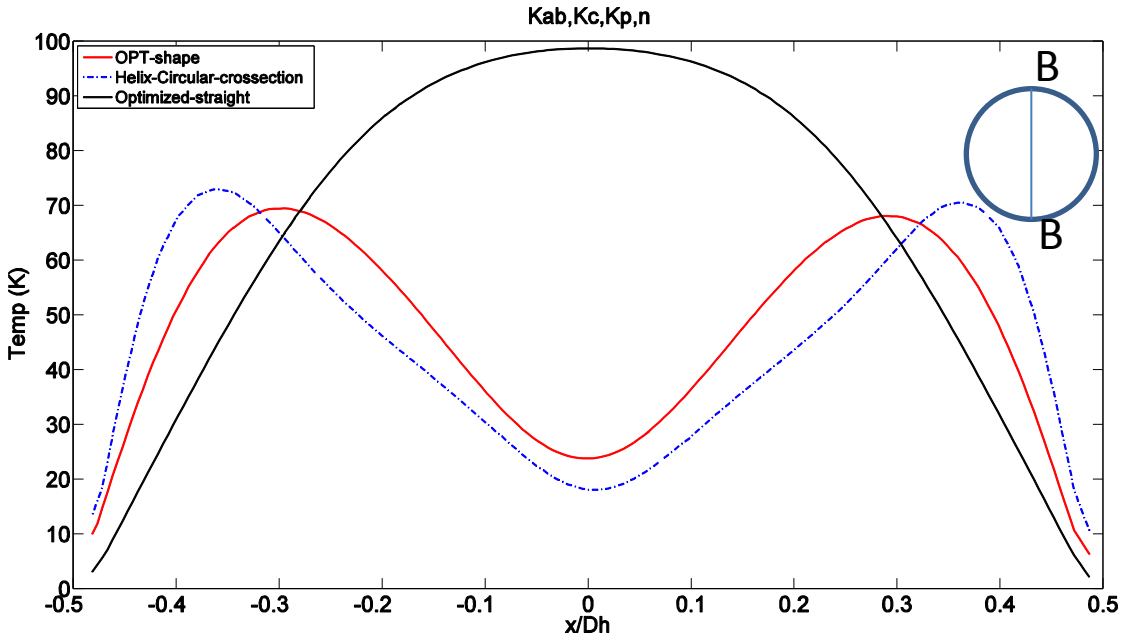

Figure 26 Temperature distribution along line BB at 95% of total length

4.2 Conclusion

From the optimization study, it can be seen that the heat transfer is sensitive to the design variables.

The non-dimensional parameters of helical coil and flow parameter are kept constant to reduce the computational time. For the optimization analysis, Re and Pr are chosen as 500 and 6.2 along with G1=30. Maximum heat transfer from the tube through the walls was achieved for the Optimized shape with design parameters are K_{ab} = 2, K_c=2.3017, K_p=3 and n=2.6438. The symmetric distribution of Temperature and helicity along the plane BB in a given cross-section at the outlet shows that the flow is developed and symmetric vortices are present, which intensifies the secondary flow causing an increase in heat transfer. The heat transfer of 47.0106w was obtained for the shape optimized design parameters. The optimized shape have 5% increment in heat transfer when compared with helical coil geometry and 45.9% increment is achieved when compared with straight tube with initial guess parameters

4.3 Future Work

1. As we see the power required for the flow to overcome the friction is sensitive to tube cross-sectional shape, we can add a pressure drop as an objective function for the optimization (Multi-objective Problem).
2. Adding twist to the helical pipe as a parameter.
3. Changing the length of the helical tube as a parameter.
4. Finding a global maxima for the objective function.
5. Continuing present work with higher Prandtl numbers.
6. Analyze the enhancement of heat transfer for different geometries like serpentine, Elongated U-bends with pitch and conical helix.
7. Unsteady flow analysis in a helical pipe.

Appendix A

Matlab Optimization output

Matlab output for Optimization Run 1

```
                                            Max     Line search  Directional  First-order
 Iter F-count        f(x)   constraint   steplength   derivative   optimality Procedure
    0       5     -61.8075            0
    1      10     -63.8622            0            1        -8.84         18.6
    2      17     -63.8804            0         0.25        -11.2         5.87
    3      22     -63.8847            0            1      -0.0617       0.0808
    4      27     -64.1299            0            1      -0.0622         13.9  Hessian modified twice
    5      33     -64.1316            0          0.5        -13.6         14.4  Hessian modified twice
    6      47     -64.1316            0      0.00195        -14.4         8.46
    7      54     -64.2507            0         0.25        -7.57      3.23e-5

Local minimum possible. Constraints satisfied.

fmincon stopped because the size of the current search direction is less than
twice the selected value of the step size tolerance and constraints are
satisfied to within the default value of the constraint tolerance.

<stopping criteria details>

Active inequalities (to within options.TolCon = 1e-06):
  lower      upper     ineqlin   ineqnonlin
                1
                3
>> Optimization stopped because the norm of the current search direction, 2.240646e-05,
is less than 2*options.TolX = 1.000000e-04, and the maximum constraint
violation, 0.000000e+00, is less than options.TolCon = 1.000000e-06.

Optimization Metric                                          Options
norm(search direction) =   2.24e-05                    TolX =   1e-04 (selected)
max(constraint violation)  =   0.00e+00                TolCon =   1e-06 (default)
```

Matlab output for Optimization Run 2

```
 Iter F-count        f(x)   constraint   steplength   derivative   optimality Procedure
    0       5     -63.8722            0
    1      15     -63.8756            0       0.0313        -17.8         42.8
    2      29     -64.0753            0       0.0625        -17.1         24.3
    3      37     -64.1148            0       0.0034        -10.4         11.46
    4      45     -64.2436            0         0.25        -7.57          7.83

Local minimum possible. Constraints satisfied.

fmincon stopped because the predicted change in the objective function
is less than the selected value of the function tolerance and constraints
are satisfied to within the default value of the constraint tolerance.

<stopping criteria details>

Active inequalities (to within options.TolCon = 1e-06):
  lower      upper     ineqlin   ineqnonlin
                1
Optimization stopped because the predicted change in the objective function,
6.001725e-05, is less than options.TolFun = 1.000000e-04, and the maximum constraint
violation, 0.000000e+00, is less than options.TolCon = 1.000000e-06.

Optimization Metric                                              Options
abs(steplength*directional derivative) =   6.00e-05       TolFun =   1e-04 (selected)
max(constraint violation) =   0.00e+00                    TolCon =   1e-06 (default)


<stopping criteria details>

Active inequalities (to within options.TolCon = 1e-06):
  lower      upper     ineqlin   ineqnonlin
                1
```

Appendix B

Size Optimization of Race Car Chassis Structure

Size Optimization of Race Car Chassis Structure

Problem Statement

The main objective of this project is to optimize a Racecar Chassis, thereby minimizing its weight using Matlab integrated with ANSYS. Therefore, for a given structure configuration and layout of beams, the optimization tool should provide the optimal structure that has Stress distribution and deflection of the beams within the constraint limit, by changing the thickness and radius of the appropriate Chassis beams while keeping Racecar weight to a minimum for a particular loading case.

Geometry and Boundary Condition

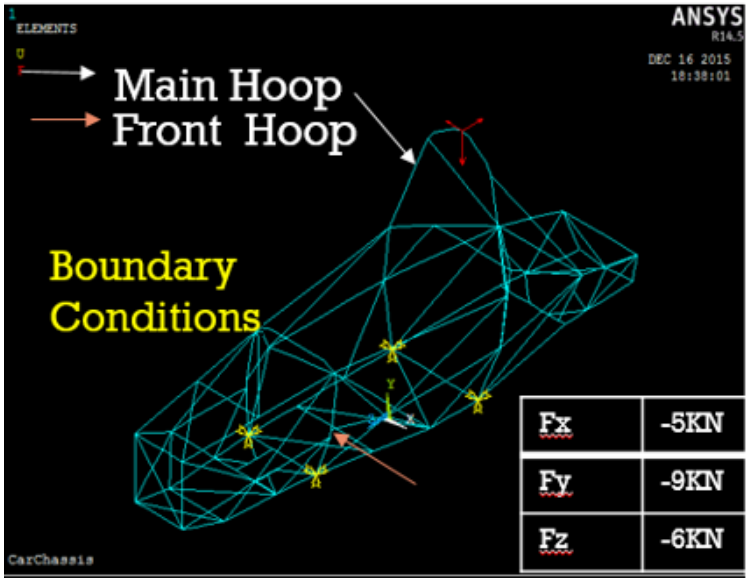

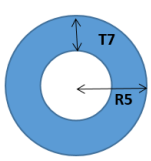

1.a- Main hoop tubes

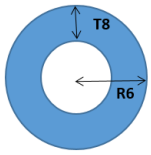

1.b- Front hoop tubes

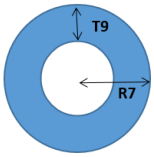

1.c- Main hoop braces

Optimized Result

Race Car Structural Component	**Design Variables**	**MATLAB**					
		Optimized Design Variable (mm)			**Weight** (Kg)		
		Active-Set Algorithm	Interior-Point Algorithm	SQP Algorithm	Active-Set Algorithm	Interior-Point Algorithm	SQP Algorithm
Main Hoop	T7	1.91	2.1	1.91	27.655	28.285	27.475
	R5	13	13	12.7			
Main Hoop Braces	T8	1.91	2.3	1.91			
	R6	14	14	13.32			
Front Hoop	T9	1.55	1.65	1.55			
	R7	13	13	12.75			

CHAPTER 5 REFERENCES

[1]. Berger, S. A., Talbot, L., & Yao, L. S. (1983). "Flow in Curved Pipes". *Annu. Rev. Fluid Mech*, *15*(1), 461-512.

[2]. Dean, W. (1928). LXXII. The stream-line motion of fluid in a curved pipe (Second paper). *The London, Edinburgh, and Dublin Philosophical Magazine and Journal of Science*, *5*(30), 673-695.

[3]. Schmidt, E. F. (1967). "Wärmeübergang und Druckverlust in Rohrschlangen". *Chemie Ingenieur Technik - CIT*, 39(13), 781-789.

[4]. Akiyama, M., & Cheng, K. (1972). "Laminar forced convection heat transfer in curved pipes with uniform wall temperature". *International Journal of Heat and Mass Transfer*, *15*(7), 1426-1431.

[5]. Prabhanjan, D., Raghavan, G., & Rennie, T. (2002). "Comparison of heat transfer rates between a straight tube heat exchanger and a helically coiled heat exchanger". *International Communications in Heat and Mass Transfer*, 29(2), 185-191.

[6]. Dravid, A. N., Smith, K. A., Merrill, E. W., & Brian, P. L. (1971). "Effect of secondary fluid motion on laminar flow heat transfer in helically coiled tubes". *AIChE Journal*, 17(5), 1114-1122.

[7]. Pawar, S., & Sunnapwar, V. K. (2014). "Experimental and CFD investigation of convective heat transfer in helically coiled tube heat

exchanger". *Chemical Engineering Research and Design*, *92*(11), 2294-2312.

[8]. Seban, R., & McLaughlin, E. (1963). "Heat transfer in tube coils with laminar and turbulent flow". *International Journal of Heat and Mass Transfer*, 6(5), 387-395.

[9]. Patankar, S. V., Pratap, V. S., & Spalding, D. B. (1974). "Prediction of laminar flow and heat transfer in helically coiled pipes". *Journal of Fluid Mechanics*, *62*(03), 539.

[10]. Akiyama Mitsunobu, & Cheng, K. (1971). "Boundary vorticity method for laminar forced convection heat transfer in curved pipes". *International Journal of Heat and Mass Transfer*, *14*(10), 1659-1675.

[11]. Jayakumar, J., Mahajani, S., Mandal, J., Iyer, K. N., & Vijayan, P. (2010). "CFD analysis of single-phase flows inside helically coiled tubes". *Computers & Chemical Engineering*, *34*(4), 430-446.

[12]. Matlab Optimization Toolbox User's Guide by The MathWorks.

[13]. ANSYS® Fluent, Release 15.0, Help System, ANSYS, Inc

[14]. Mori, Y., & Nakayama, W. (1967). "Study on forced convective heat transfer in curved pipes". *International Journal of Heat and Mass Transfer*, 10(5), 681-695.

[15]. Austen, D., & Soliman, H. (1988). "Laminar flow and heat transfer in helically coiled tubes with substantial pitch". *Experimental Thermal and Fluid Science*, 1(2), 183-194.

[16]. Zapryanov, Z., Christov, C., & Toshev, E. (1980). "Fully developed laminar flow and heat transfer in curved tubes". *International Journal of Heat and Mass Transfer*, 23(6), 873-880.

[17]. Yang, G., Dong, Z., & Ebadian, M. (1995). "Laminar forced convection in a helicoidal pipe with finite pitch". *International Journal of Heat and Mass Transfer*, 38(5), 853-862.

[18]. Sillekens, J. J., Rindt, C. C., & Van Steenhoven, A. A. (1998). "Buoyancy-induced secondary vortices in the entrance section of a horizontal straight tube". *Numerical Heat Transfer, Part A: Applications*, 33(4), 355-369.

[19]. Williams, G. S., Hubbell, C. W., Fenkell, G. H. 1902. "Experiments at Detroit, Mich., on the effect of curvature upon the flow of water in pipes". *Trans. ASCE* 47:1-196

[20]. M. Sukri, M. Ali, C. J. Doolan, and V. Wheatley, "Grid Convergence Study for a Two-Dimensional Simulation of Flow around a Square Cylinder at a Low Reynolds Number," *Seventh Int. Conference CFD Miner. Process Ind. CSIRO*, no. December, pp. 1–6, 2009.

[21]. Jasbir S. Arora. (2004). "Introduction to Optimum Design", v.

[22]. Roache, P. J., & Knupp, P. M. (1993). Completed Richardson extrapolation. Communication in Numerical Methods in Engineering, *9*(5), 365-374.

[23]. Carrigan, T. J., Dennis, B. H., Han, Z. X., & Wang, B. P. (2012). "Aerodynamic Shape Optimization of a Vertical-Axis Wind Turbine Using Differential Evolution". *ISRN Renewable Energy*, 1-16.

[24]. Zhao, H., Chen, G., & Zhou, J. Z. (2012). "The Robust Optimization Design for Cylindrical Helical Compression Spring". *AMR*, 433-440, 2201-2205.

[25]. Taktak, M., Omheni, K., Aloui, A., Dammak, F., & Haddar, M. (2014). "Dynamic optimization design of a cylindrical helical spring". *Applied Acoustics*, 77, 178-183.

CHAPTER 6 BIOGRAPHICAL INFORMATION

Manoj V Kandukuri was born in Hyderabad, India. Did his bachelors in technology in Aeronautical Engineering from IARE, a JNTU affiliated College in Hyderabad, India (2009). He holds a Master's degree in Aerospace Engineering from University of Manchester, U.K (2010). His Thesis topic was "Effect of roughness of jets in high speed cross flow", where he analyzed the roughness effects on Aerodynamic characteristics and architecture of the flow field with 2 different jet cross flows at high speeds experimentally. After his graduation, he worked as CFD aero-data engineer in Defense Research and Development Laboratories India for 2 years. His main responsibilities was to analyze the external aerodynamic stability and control for cruciform re-entry vehicles. He then came to US to purse an MS degree program in Mechanical Engineering at University of Texas at Arlington. His research interest include optimization and Fluid Structure Interaction. He is currently working as an Application Engineer Intern at Altair Engineering Inc. Houston, USA.